Ring-diffusion mediated homogeneous melting in the superheating regime

Xian-Ming Bai* and Mo Li†
School of Materials Science and Engineering, Georgia Institute of Technology, Atlanta, Georgia 30332-0245, USA
(Received 11 January 2008; revised manuscript received 3 March 2008; published 18 April 2008)

Homogeneous melting in the superheating regime is investigated by using molecular dynamics simulation of a Lennard-Jones model system. We show that the commonly observed catastrophic melting at the superheating limit is caused by fast heating rate. By keeping the system isothermally at temperatures below the superheating limit, we observe intense self-diffusion motions as the precursor of melting. The highly correlated atomic motions are related to the self-diffusion loops or rings. Two types of loops are observed, closed loop and open loop, where the latter is directly related to the homogeneous nucleation of the liquid phase. Homogeneous melting occurs when the number density of diffusion loops reaches a critical value. Our results suggest that homogeneous melting in the superheating regime is a first-order thermodynamic phase transition triggered by the self-diffusion loops when the kinetic constraint imposed by heating rate is lessened.

DOI: 10.1103/PhysRevB.77.134109 PACS number(s): 64.70.D−, 61.72.Bb, 66.10.C−, 87.10.Tf

I. INTRODUCTION

Melting is commonly observed but also one of the least understood phenomena in nature. When the temperature reaches the melting point, heterogeneous melting usually occurs at defect sites in solids, such as surfaces, grain boundaries, and interfaces.[1] The heterogeneous melting can be explained satisfactorily through the thermodynamic relation among the interface energies. Namely, the sum of the newly formed solid-liquid and liquid-vapor interface energies is less than or equal to the solid-vapor interface energy, or $\gamma_{sv} \geqslant \gamma_{sl} + \gamma_{lv}$, where s, l, v represent solid, liquid, and vapor phases, respectively.[1] The decrease in the total (interfacial) free energies is the cause for the heterogeneous melting. However, how a liquid nucleates in a perfect (i.e., surface-free and defect-free) crystal remains an open question to date. Specifically, the detailed microscopic mechanisms and the thermodynamic relations of this seemingly simple phenomenon still remain unanswered, despite extensive studies made in the past century.[2–21]

The difficulties originated mainly from the presence of surfaces. Since all materials have surfaces and the preemptive heterogeneous surface melting is always dominant, homogeneous melting could not occur without superheating the solids.[4,7,8] Nevertheless, in several cases, superheating was indeed achieved when special techniques were used to suppress the surface melting. For example, Daeges *et al.*[9] coated a silver sphere with a thin layer of gold. Since the lattice constants of gold and silver are very close, coating (or preferably epitaxially growing) gold is tantamount to removing the free surface of the silver particle. Because the melting temperature of gold is higher than that of silver, the coated silver core would melt earlier than the gold shell. As a result, up to 25 K of superheating above the normal melting point in the silver was observed for a time period of about 1 min. Superheating can also be achieved by using picosecond pulsed laser irradiation techniques.[10–14] The laser irradiation heats the materials internally and therefore can initiate melting from the bulk, or homogeneously. Substantial superheating (about 20% above the normal melting point) has been observed from these experiments. However, melting is extremely fast in these experiments, typically, in just a few nanoseconds. Thus, many kinetic and thermodynamic parameters could not be precisely measured or controlled. Consequently, it is difficult to investigate the detailed microscopic mechanisms of homogeneous melting in the superheating regime from these experiments. Recently, computer simulations[15–19,21] have been used for investigating homogeneous melting. By employing periodic boundary conditions, one can "remove" surfaces, so superheating can be achieved easily. However, the heating rates are extremely high in most simulations,[15–19,21] usually on the order of 10^{11}–10^{13} K/s. Under such high heating rates, melting is always observed to occur catastrophically. Due to the short time window (e.g., a few hundred femptoseconds) available in the catastrophic melting, many vital kinetic and thermodynamic properties are suppressed. As a result, the detailed microscopic mechanism and kinetic behavior related to homogeneous melting are either missed or only partially accessible.[15–19,21]

In this paper, we investigate the microscopic mechanism of homogeneous melting in the superheating regime by using molecular dynamics simulation. The baseline of this study begins at the heating rate effects on melting. We show that while the fast *heating rate* leads to catastrophic melting at the *superheating limit*, slow heating rate can lead to more detailed observations of the thermodynamic and, in particular, the kinetic processes at temperatures *below* the superheating limit. To this end, an isothermal heating method is implemented (see Sec II A for the explanation). Detailed information will be examined at fixed temperatures before and after melting occurs by monitoring various structural and defect characterization quantities, thermodynamic properties, kinetic behaviors, and atomic movements. In particular, we focus on the correlated atomic motions under the isothermal heating condition and their relation to local disorder or liquid nucleus formation. Our results reveal that strong diffusive atomic motions occur in a quiescent period before melting occurs, which have been missed in the fast heating process. The highly correlated motions consist of both closed and open loops of self-diffusing atoms. It is the open loops that eventually lead to the formation of liquid nuclei. The thermodynamic and kinetic properties obtained from this work allow us to probe into the atomic mechanisms of homoge-

neous melting with deeper physical insights. Our results suggest that homogeneous melting in the superheating regime is a first-order thermodynamic phase transition triggered by the atomic motions in the form of the diffusion loops when the heating rate is kept sufficiently low.

This paper is organized as follows. In Sec. II, we outline the simulation methods and procedures used in this study. In Sec. III, we present our simulation results. Our focus will be on the structural and thermodynamic properties and diffusive motions of atoms under isothermal heating condition. In Sec. IV, we discuss the results with particular attention paid to the evolution of the liquid phase nucleating from the superheated solid. The nature of the homogeneous melting will also be discussed in light of these results and compared with some previously proposed models. Finally, we summarize the results and present the conclusions drawn from this work.

II. METHODS

A. Molecular dynamics simulation and system parameters

In this work, we use a perfect crystal to investigate the homogeneous melting. Initially, all atoms are arranged in an fcc lattice. The periodic boundary conditions are employed in all directions. Therefore, the system is both surface-free and defect-free. The atoms interact via a standard Lennard-Jones (LJ) potential for solid argon, $\phi(r)=4\varepsilon[(\sigma/r)^{12}-(\sigma/r)^{6}]$, where $\varepsilon=119.8k_B$ and $\sigma=3.405$ Å. The temperature unit is in $\varepsilon/k_B\approx 120$ K. The cutoff distance is set to 2.5σ. Molecular dynamics (MD) simulations are performed in an ensemble with constant number of atoms, constant pressure, and constant temperature, or *NPT* ensemble. The Parrinello-Rahman method[22] is used to control the system volume; and the Nose thermostat[23] is used to control the system temperature. The pressure of the system is kept at zero in all simulations. The MD time step was set to 5×10^{-15} s. As a widely used convention,[24] all quantities of the system are in the reduced LJ units scaled by σ, ε, and the mass of argon m (=39.95 amu$=6.634\times10^{-26}$ kg).

For this model system, the equilibrium melting temperature is at $T_m^E=0.618$ (in reduced LJ unit, ε/k_B), which is obtained by monitoring the liquid-solid interface motion in the coexisting liquid and solid phases.[25] The equilibrium melting point is the transition temperature of the (heterogeneous) surface melting, which, for historical reasons, is called the normal melting point of a solid. To obtain homogeneous melting, however, it requires us to remove the surfaces or interfaces, which can be accomplished by using the periodic boundary conditions in computer simulations.

Heating rate is a crucial parameter that directly affects the nature of homogeneous melting. There are two ways for heating the sample: gradual heating (GH) and isothermal heating (ISH). The GH method can be described as "heat until it melts."[26] In this method, one heats the sample continuously from a low temperature to a high temperature with a constant heating rate until the sample melts. Previously, researchers have made almost exclusive use of this method for investigating homogeneous melting.[15–19] Due to the inherent time-scale limitation in MD simulations, the typical heating rate in the GH method is normally on the order of $10^{11}-10^{13}$ K/s which is much faster than the heating rate in reality. The fast heating rate may suppress the kinetic processes in homogeneous melting, which we will explain in detail later in Sec. III A. To overcome this problem, we employ the ISH method. In this method, the heating process has two distinct steps. First, we heat the system from a low temperature to a desired high temperature within the superheating regime at which melting has not occurred yet. So this step is the same as the GH method mentioned above. Next, at this temperature, the heating process is stopped and the system temperature is held isothermally (constant) for an extended time period (e.g., millions of MD steps). We should mention that the temperature is not strictly constant during this period; it fluctuates slightly around the desired temperature because of the thermal noises. This method allows the system to have sufficient time to explore the phase space and execute kinetic motions that are critical to the thermodynamic phase transitions. Of course, very slow heating rate can be used, such as in the work of Forsblom and Grimvall[20] (e.g., 1.9×10^{10} K/s, or about 2 K for every 50 000 time steps, where 1 time step$=2.1\times10^{-15}$ s), if one knows the characteristic time scale in the kinetic process such as diffusion. In such cases, the GH and ISH should give the same results.

In Sec. III A, we show that the fast heating rate of the gradual heating as employed in other MD simulations leads to catastrophic melting at the highest temperature T_m^S in comparison with isothermal heating. Melting occurring at this temperature is fast or spontaneous. Usually, T_m^S is called the upper limit of superheating. For our LJ system, T_m^S is around 0.76 in the GH method. In other words, the maximum superheating is $T_m^S-T_m^E=0.142$, or about 23% above the equilibrium melting point for the Lennard-Jones model system. This value is in good agreement with many previous results reported in the literature.[16,18,19,21]

B. Structure characterization

Melting of a crystal is a topologically order-to-disorder transition. During melting, the crystal loses its long-range translational order and becomes a liquid with a disordered structure. The structural change can be monitored, among other ways, by pair distribution functions (PDFs). PDFs describe the average atom densities at different interatomic distances.[24] Because they can be measured from x-ray diffraction or other scattering experiments, PDFs are very useful for differentiating the structures in crystal and liquid states. So using PDFs, one can compare the simulation and experiment directly. For a monatomic system, the PDF can be calculated straightforwardly in a simulation as

$$g(r)=\frac{V}{N^2 4\pi r^2 dr}\sum_{i=1}^{N}\Delta N_i(r), \tag{1}$$

where V is the volume of the total system, N is the total number of atoms in the system, and $\Delta N_i(r)$ is the number of atoms in a shell between the distance r and $r+dr$ from the position of atom i. For each atom, we can calculate the atom densities at different distances from it, and the PDF is the

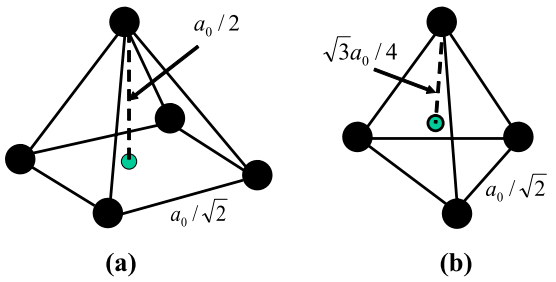

FIG. 1. (Color online) Two types of interstitial sites in fcc crystals. The distance between the interstitial site [filled circle in green (gray)] and its nearest atom (filled circle in black) is indicated by a dashed line in each figure, where a_0 stands for the lattice constant. (a) Octahedral site and (b) tetrahedral site.

average of this density over all the atoms. In addition, we use direct visualization which is very valuable when other quantitative methods, including the PDF, become insufficient.

C. Defect characterization

Number of the first nearest neighbors (1NNs). The presence of structural defects is an integral part of melting transition when a crystal is heated toward the melting point. The number of the 1NNs is an important characteristic of the crystal symmetry. It is also closely related to many structural defects and transport properties. A missing nearest-neighbor atom could form a vacancy that is thought to play an important role in melting.[5] For a perfect fcc crystal, the 1NN number is 12. If the crystal structure changes, it becomes different. In some previous papers,[17,27,28] the authors defined an atom as a defective atom if the number of its 1NNs is not 12. In this work, we find that this definition leads to a higher upper bound. Based on the statistical measurement of the 1NN distribution in a pure liquid whose average number of 1NN is 9.4 (see detailed information in Sec. III C), we define an atom as being "liquidlike" when it has nine or less nearest neighbors. When the temperature is high, thermal fluctuations can aggregate the defective atoms to form clusters, some of which are thought to form "dislocation lines" or "dislocation loops" in some previous studies.[17,27–29] To calculate the number of the 1NNs, we use the critical cutoff distance at which the PDF reaches its first minimum. We chose the base value as 1.33σ at $T=0.2$ and adjusted it according to the lattice expansion at different temperatures.

Interstitial defects. The interstitial defects can play an important role in melting.[20,30–34] If an atom inside a solid jumps from a lattice site to an interstitial site, it could create an interstice-vacancy pair. The interstitial atom intends to push the surrounding atoms away from their equilibrium sites. Thus, an interstitial defect is in a high-energy state and can cause serious disordering or instability to the crystal. Forsblom and Grimvall[20,30] have shown that a cluster of ten interstice-vacancy pairs can trigger melting in aluminum. For fcc crystals, there are two types of interstitial sites: octahedral site [Fig. 1(a)] and tetrahedral site [Fig. 1(b)].[35] The minimum distance between an octahedral site and its nearest atom is $r_{oct\text{-}atom}=a_0/2$, while the minimum distance between a tetrahedral site and its nearest atom is $r_{tet\text{-}atom}=\sqrt{3}a_0/4$, where a_0 is the lattice constant of the fcc crystal. If an atom is sitting on an interstitial site, then the distance between this atom and its nearest neighbor should be close to either $r_{oct\text{-}atom}$ or $r_{tet\text{-}atom}$, depending on the type of the interstitial site it occupies. In our simulation, by searching the minimum interatomic distance among all atom pairs during melting process, we can identify the interstitials: if the distance is close to $r_{oct\text{-}atom}$, there may be an octahedron interstitial, or if it matches $r_{tet\text{-}atom}$, there may be a tetrahedron interstitial. Another possible outcome is that the minimum distance is much larger than either $r_{oct\text{-}atom}$ or $r_{tet\text{-}atom}$. In such case, the interstitial defect may not form.

Vacancies and dynamic 1NN disorder. When an atom is missing from the lattice site, an open space forms, which suggests that by using the 1NN number we may define a vacancy. However, a vacancy should also have a long lifetime. Therefore, this open space is not necessarily a stable vacancy. If its lifetime is as long as a few nanoseconds, we should treat it as a vacancy. If it only lasts for a short time period, such as a few hundred femptoseconds, we define it as dynamic 1NN disorder. As shown below, the dynamic 1NN disorder plays an important role in homogeneous melting.

D. Mean square displacement

From the atomic point of view, melting basically involves atoms moving away randomly from their equilibrium lattice positions under thermal agitation so that a crystal loses its translational order. The atomic displacement is a key parameter for characterizing and understanding the melting process. The mean square displacement (MSD) can be calculated by taking the average of the square displacement over all atoms in the system,

$$S^2(t) = \frac{1}{N}\sum_{i=1}^{N} |\vec{r}_i(t) - \vec{r}_i(0)|^2, \tag{2}$$

where $\vec{r}_i(0)$ stands for the initial (or equilibrium) position of atom i at time 0 and $\vec{r}_i(t)$ represents the new position at time t. Lindemann theory[3] considers that the MSD is mainly contributed from the lattice vibration. It states that when the *vibrational* root mean square displacement (RMSD) exceeds a critical value, melting occurs. Typically, the critical RMSD is about 20% of the nearest-neighbor distance.[3,16] However, as we show in Sec. III B, diffusive motions of atoms also induce atomic displacement, which can become significant at high temperatures in the superheating regime. Under certain conditions, the system does not melt even though the RMSD is much larger than the critical value. It is this realization of the *diffusive* MSD that led us to focus on the use of isothermal heating and the discovery of the connection between homogeneous melting and the self-diffusion.

III. RESULTS

A. Heating rate effects: Gradual heating versus isothermal heating

In order to test the heating rate effects on melting at superheating, we use both the GH and ISH methods to heat a

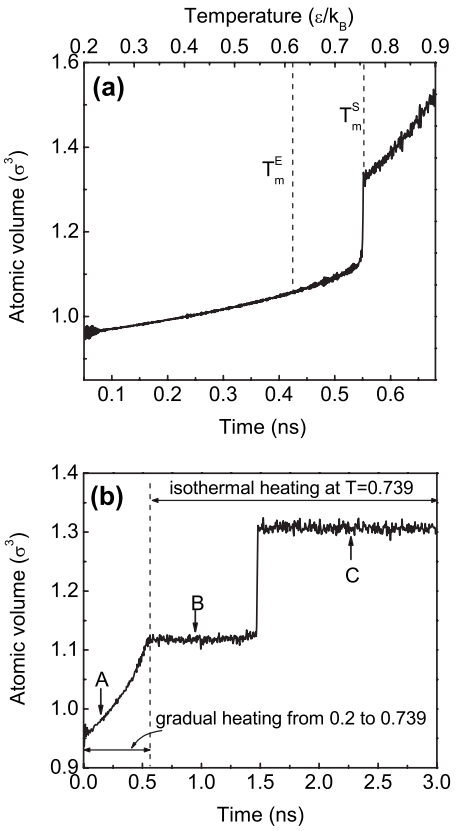

FIG. 2. Atomic volume change during melting in gradual heating and isothermal heating methods. (a) Gradual heating method. The bottom x axis shows the time from the beginning of the simulation, and the top x axis shows the corresponding temperature at each time. T_m^E stands for the normal (or equilibrium) melting point and T_m^S represents the upper limit of superheating obtained at high heating rate. (b) Isothermal heating method. The isothermal heating starts at $T=0.739$. Three moments (marked by A, B, and C) are picked for investigation in Figs. 3 and 4.

crystal sample of 4000 atoms. (Note that a smaller system of 500 atoms is also used for the purpose of easy visualization and short simulation time. We shall make note for these cases when they occur.) Figure 2(a) shows the melting process under the GH condition. The sample is heated continuously from $T=0.2$ (=24 K) to 0.9 (=108 K) with a heating rate of 1.33×10^{11} K/s (where T increases 0.2 K every 300 MD steps). As the temperature increases, the system volume expands. At $T=0.76$ (or after 0.55 ns), the system volume jumps to a larger value, indicating that melting occurs at this temperature. This temperature is usually called the upper limit of the superheating, T_m^S. In most previous studies,[16–19] the GH method was used to determine T_m^S.

For most solids, the typical lattice vibration frequency is about 10^{12}–10^{14} Hz. Generally, to achieve full relaxation or thermal equilibration for atomic configuration at a given temperature, hundreds to thousands of cycles of lattice vibration are needed, which corresponds to about 10^{-10}–10^{-12} seconds, or 10^3–10^5 MD steps in a typical MD simulation (1 MD step=5×10^{-15} s in our system). In the superheating regime, the lattice vibration frequency becomes lower,[35] typically by at least an order of magnitude, and thus the minimum time needed for relaxation is an order of magnitude higher. However, under extremely high heating rate in MD simulation (e.g., 10^{11} K/s or higher), the allowed relaxation time at each temperature is only about 10^3 MD steps or less, which may become insufficient for the relaxation. Additionally, as revealed by this work, the relaxation time is further constrained by the diffusion motion needed to reach melting at each fixed temperature, which could be millions of MD steps (see Sec. III B). Therefore, the atoms have little time to sample the phase space at each temperature before the system is elevated to a new temperature. This serious lack of relaxation is usually manifested as strong hysteresis at the melting temperature. In other words, the system is simply ushered to the limit of the superheating, T_m^S. Therefore, only transient thermodynamic properties can be obtained at the temperatures toward T_m^S. Moreover, the kinetic processes, in particular, the atomic movements, which are important for understanding the detailed microscopic mechanisms of melting, are hindered or suppressed because the atoms are not given enough time to relax (or move afar). Indeed, as shown in Sec. III D, the complex diffusion motions will not be fully revealed if the isothermal heating method (or slow heating rate[20]) is not used.

To overcome this fundamental limitation, we employed the isothermal heating method. As we mentioned in Sec. II A, first, the GH method is used to bring the system to a specific temperature in the superheating regime, and then the heating process is stopped and the system is held isothermally at this temperature for a long period of time (up to 10^6–10^7 MD steps), which amounts to an infinitely slow heating rate at this temperature. Figure 2(b) shows the melting process using the ISH method. First, the system is heated from 0.2 to 0.739, which is about 3% below T_m^S (=0.76), with a heating rate of 1.33×10^{11} K/s. Then, at $T=0.739$, the gradual heating is stopped and the system is held isothermally. At the beginning of the isothermal regime, the system is still in the crystalline state. After about 1.4 ns, the system volume increases suddenly, indicating that the system transforms from crystal state to liquid state. Therefore, keeping the system isothermally would lead to lower homogeneous melting temperatures that fall within the superheating regime below T_m^S.[36] Using the ISH method, we find a quiescent or incubation period when melting can occur at lower temperatures below T_m^S. Figure 2(b) shows that the time needed to observe melting increases dramatically as the isothermal temperature becomes lower. This quiescent period could last millions of MD steps or longer depending on how far the temperature is from T_m^S. (This is also why we only focused on a few temperatures slightly below T_m^S in this study.) In contrast, there is no such quiescent period observed in gradual heating with high heating rate. Thus, using the GH with high heating rate would surely miss the important kinetic information in the quiescent period.

In Fig. 2(b), we pick three representative times for investigation: time A at $T=0.3$ in the gradual heating period, time B at $T=0.739$ in the isothermal regime and before melting occurs, and time C at $T=0.739$ in the isothermal heating regime but after melting occurs. In Fig. 3, we show the snapshots (two-dimensional (2D) projections along the [100] direction) of the atomic configurations at these times, and in

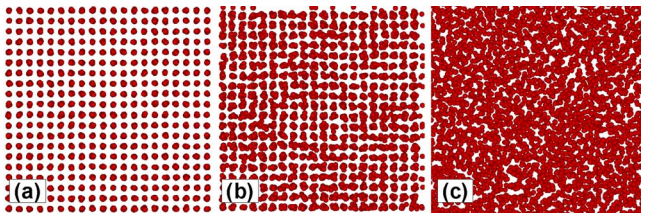

FIG. 3. (Color online) Two-dimensional projected snapshots of the atomic configurations along the [100] direction at the three times marked in Fig. 2(b). (a) At time A, $T=0.3$; (b) at time B, $T=0.739$ and before melting occurs; and (c) at time C, $T=0.739$ and after melting occurs.

Fig. 4 we show the corresponding PDFs. At time A where the temperature is still low, the atoms vibrate around their equilibrium sites and the structure is nearly a perfect fcc crystal [Fig. 3(a)]. The PDF at this temperature (Fig. 4) has very sharp peaks. The distance at which the first peak reaches its minimum is used as the cutoff distance for locating the 1NNs at this temperature. At time B where the melting has not occurred in the isothermal regime, some atoms are disordered but the overall crystal structure still remains [Fig. 3(b)]. The crystal peaks of the PDF at this temperature become broader, but one is still able to identify them. At time C where the melting has occurred, most atoms have moved away from their equilibrium sites and the system becomes a liquid [Fig. 3(c)]. Most peaks in the PDF disappear and approach the uniform atomic density at large interatomic distance. There is, therefore, a long incubation time before melting occurs in the isothermal regime, during which the system still keeps the crystal symmetry, despite large distortions. As shown below, this quiescent period provides a valuable window for us to investigate the kinetics and detailed atomic motions leading to the final melting.

B. Atom movements

Melting is a spatial transition with atoms moving away randomly and permanently from their equilibrium lattice positions under thermal agitation. There are two types of displacements in the thermally agitated crystals, vibrational and diffusive displacements. The former was recognized earlier by Lindemann[3] in relation to melting. The criterion named after him states that a crystal becomes a liquid when the ratio of the RMSD of the vibrating atoms to the average nearest-neighbor distance reaches a critical value, which is usually around 0.2 for most metals.[21] With the MD simulation in conjunction with the isothermal heating, we can look into more detailed atomic movements in the superheating regime other than just the MSD from lattice vibrations. The information will furnish the basis for our understanding of microscopic mechanisms of homogeneous melting.

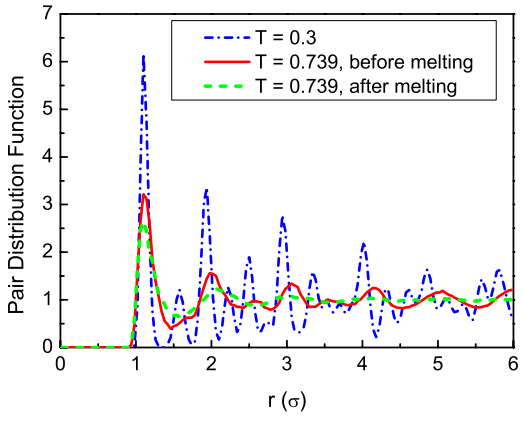

FIG. 4. (Color online) Pair distribution function (PDF) at the three times marked in Fig. 2(b). Blue (black) short dash dot line: $T=0.3$ (time A). (b) Red (dark gray) solid line: $T=0.739$ and before melting occurs (time B). (c) Green (light gray) short dash line: $T=0.739$ and after melting occurs (time C).

We have calculated the MSD under both the gradual heating and isothermal heating conditions. It is worth noting that the reference atom positions for calculating the MSD should be adjusted with temperature as the system volume expands at each elevated temperature. In this work, the reference positions are the perfect fcc lattice sites. The lattice constant of the reference lattice at each temperature is calculated from the temperature-dependent crystal volume:

$$a_0 = [4V(T)/N]^{1/3}, \tag{3}$$

where $V(T)$ is the fcc crystal volume at temperature T from the MD simulation and N is the number of atoms in the system.

In the GH case, the system temperature increases continuously from 0.2 to 0.8 with a heating rate of 1.33×10^{11} K/s. Figure 5(a) shows the MSD during the gradual heating as a function of both time (bottom x axis) and temperature (top x axis). The rapid increase of the MSD at 0.55 ns ($T=0.76$ accordingly) indicates melting transition. The critical MSD for melting [indicated by the arrow in Fig. 5(a)] is about $0.04\sigma^2$. So the RMSD, Δr_{RMSD}, is about 0.2σ. At $T=0.76$, the average volume per atom, Ω, is about $1.13\sigma^3$, so that the average first nearest-neighbor distance is $r_{NN}=2^{-1/2}(4\Omega)^{1/3}=1.17\sigma$. Thus, the critical Lindemann ratio for melting is $\delta_L^*=\Delta r_{RMSD}/r_{NN}=0.171$, which is in good agreement with the previous result.[16] So the Lindemann criterion appears to be satisfied in the GH method.

In the ISH case, the system temperature is held isothermally at $T=0.738$. Note that at $T=0.739$, a homogeneous melting occurs after 1.45 ns in the isothermal period, as shown in Fig. 2(b). However, at $T=0.738$ in the isothermal regime, the sample does not melt for at least 3.5 ns (about 700000 MD steps). It may be possible to observe melting at this temperature or even lower temperatures if the simulation time is sufficiently long. However, the long simulation time needed for observing melting at lower temperatures exceeds our computing capacity. Thus, in this work, we treat the system at $T=0.738$ as a nonmelting system within the achievable simulation time. In addition, we performed several runs for the systems with different initial conditions. For all the simulations, melting occurs at 0.739 but does not at 0.738 within 3.5 ns isothermal period. The incubation time before melting, however, is found to range from 0.33 to 1.5 ns at $T=0.739$. So the mean time is around 0.90 ns in a statistical sense. The calculated MSD as a function of time is shown in Fig. 5(b). The isothermal condition is set after about 0.55 ns

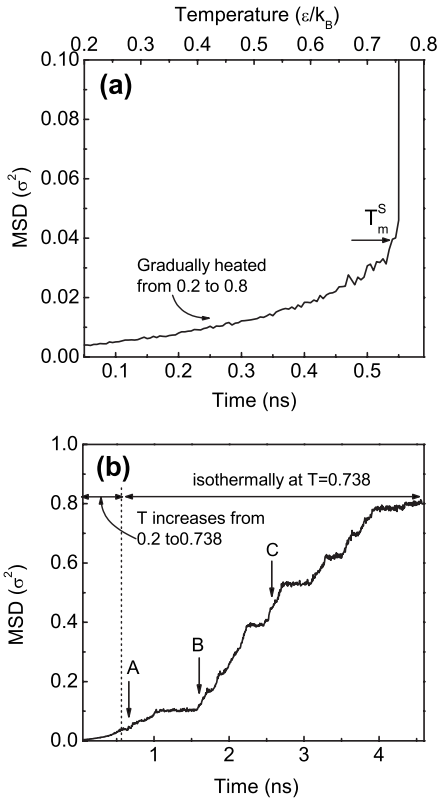

FIG. 5. Mean square displacement (MSD) in both gradual heating and isothermal heating methods. (a) Gradual heating. The bottom x axis is the time, and the top x axis is the temperature. The upper superheating limit is marked by T_m^S. (b) Isothermal heating method. The isothermal heating starts at $T=0.738$. No melting was observed in the isothermal regime despite of the large MSD. Three times (A–C) are picked for investigation in Fig. 6.

from the beginning of the simulation. In the isothermal regime, the MSD keeps increasing with time. At the end of the simulation (4.6 ns), the MSD is about $0.8\sigma^2$, which is much larger than the critical value predicted from the Lindemann criterion ($\sim 0.04\sigma^2$). In addition, there are sporadic increases in the MSD that, as we discuss in Sec. III D, are from correlated atomic motions. It is worth noting again that during the entire isothermal heating, the system still remains in crystalline state. Therefore, the Lindemann criterion is not satisfied under the ISH condition, which is quite different from the GH case.

More detailed information can be obtained regarding the movements of the atoms that contribute to the extraordinarily large MSD at $T=0.738$. To do so, in Fig. 6, we plot the distributions of the atomic displacements at three times marked by A–C in Fig. 5(b). The displacement distribution function measures the fraction of the atoms that travel a distance r at an elapsed time from their original equilibrium sites. Note that the original equilibrium sites are obtained by averaging atom positions over the first 0.025 ns period in the isothermal regime. Then, we calculated the distributions at three elapsed times: (a) time A after 0.025 ns isothermal run (right after obtaining the equilibrium atomic positions), (b) time B after 1 ns isothermal run, and (c) time C after 2 ns isothermal run. Distribution (a) shows that the first (main)

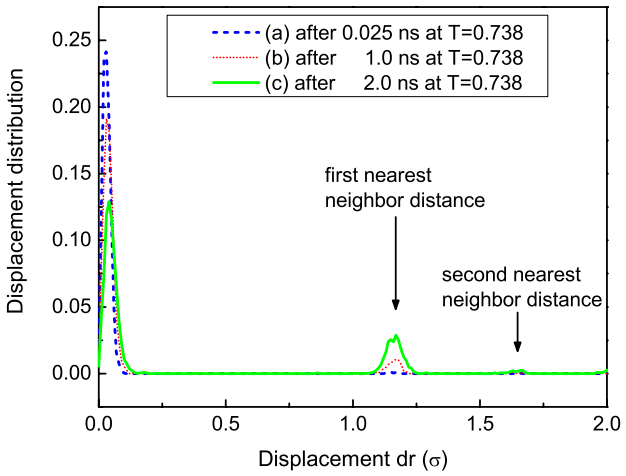

FIG. 6. (Color online) Distributions of the atom displacements at different times [marked by A, B, and C in Fig. 5(b)] in the isothermal regime. The time is scaled to zero at the beginning of the isothermal regime. Blue (black) short dash line: after 0.025 ns from the beginning of isothermal heating; red (dark gray) short dot line: after 1.0 ns; green (light gray) solid line: after 2.0 ns.

peak is very sharp and its center is at $r \approx 0.03\sigma$, which is about 2.6% of the first-nearest-neighbor distance, indicating that all atoms vibrate around their original equilibrium sites at that time. After 1 ns isothermal run, Distribution (b) shows that the height of the first peak decreases to a certain extent and the width increases slightly. Overall, most atoms still vibrate around their original sites with very small displacements. However, one can find that some atoms have traveled a distance of about 1.15σ, as indicated by the arrow at the second peak in Fig. 6. This displacement is very close to the first-nearest-neighbor distance, $\sqrt{2}/2a_0 \approx 1.16\sigma$ (where $a_0 \approx 1.647\sigma$ at $T=0.738$), implying that some atoms have hopped to their first neighboring lattice sites. After 2 ns isothermal run, the height of this peak increases in distribution (c), indicating that more atoms have traveled to their first neighboring sites. Moreover, another peak appears at $r \approx 1.64\sigma$, which is very close to the second-nearest-neighbor distance, $a_0 \approx 1.647\sigma$, indicating that some atoms have made a second-order hopping from their first-nearest-neighbor sites.

The above results clearly show that diffusion is a major foreplay in the quiescent period before homogeneous melting occurs. The Lindemann criterion derived from lattice vibration is therefore inadequate in predicting homogeneous melting under the isothermal heating or low heating rate condition. In order to reveal the connection between the long-range diffusive motion and melting itself, more detailed characterization of defects is needed.

C. Defect process

For atoms to hop or diffuse in a crystal, some extra open spaces are needed. These spaces can be vacancies, interstitial sites, or, as shown below, dynamic 1NN disorder. Since the initial crystal is perfect in our simulation, the atomic hopping must be helped with some thermally activated defects with

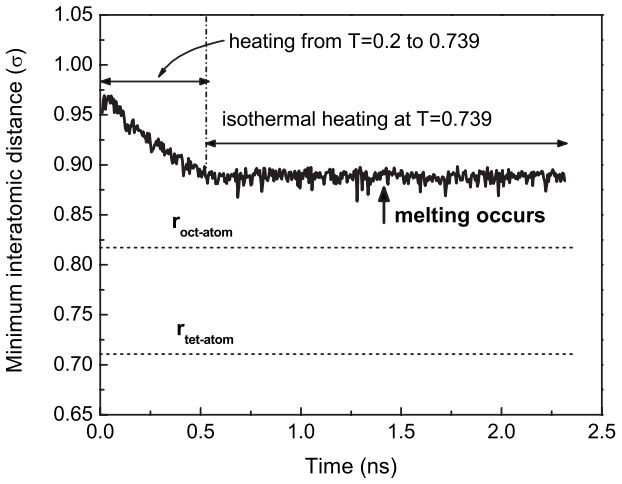

FIG. 7. The shortest interatomic distance as a function of time during the isothermal heating at $T=0.739$. The ideal distance between an octahedral interstitial site and its neighboring atom is indicated by $r_{oct\text{-}atom}$, and that between a tetrahedral interstitial site and its neighboring atom is indicated by $r_{tet\text{-}atom}$.

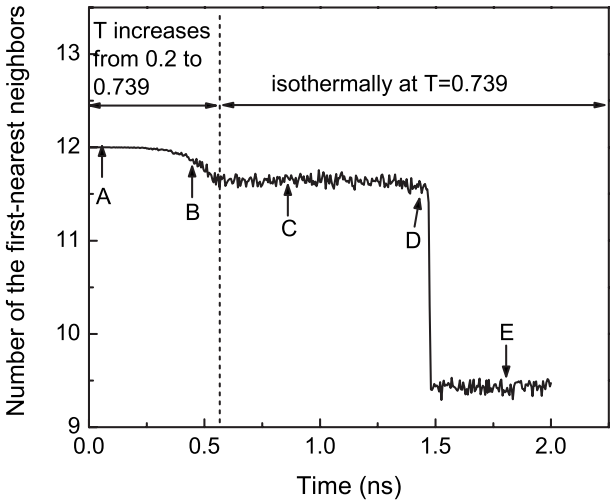

FIG. 8. Evolution of the average number of the first nearest neighbors during the isothermal melting process at $T=0.739$. Five times (A–E) are picked for investigation as shown in Fig. 9.

open spaces. The first candidate is the interstitial. In Sec. II C, we have discussed that the interstitial can be identified from the characteristic distance between an interstitial site and its nearest lattice atom. As shown in Fig. 1, the distance between an octahedral site and its nearest atom is $r_{oct\text{-}atom}=a_0/2$, and that between a tetrahedral site and its nearest neighbor is $r_{tet\text{-}atom}=\sqrt{3}a_0/4$. At $T=0.739$ (note that melting eventually occurs in the isothermal regime at this temperature), the average crystal lattice constant is $a_0\approx 1.647\sigma$. Therefore, the respective characteristic distances are $r_{oct\text{-}atom}=0.82\sigma$ and $r_{tet\text{-}atom}=0.71\sigma$. Prior to melting, if the thermal fluctuations generate an interstitial defect, the minimum distance between the defective (interstitial) atom and its surrounding atoms should be close to one of the characteristic interstitial-atom distances.

In order to check whether some atoms occupy the interstitial sites before melting, we did the following investigation. We heated a perfect crystal from $T=0.2$ to 0.739 and then held the system isothermally at this temperature, and the heating procedure is shown in Fig. 2(b). At $T=0.739$, initially the system is in the crystal state and finally becomes a liquid after 1.4 ns. During this process, we calculated the interatomic distances of *all pairs* of the atoms in the system at every MD step and subsequently sorted out the *shortest* distance among all pairs. The minimum interatomic distance is logged during this process as shown in Fig. 7. As the temperature increases, the shortest interatomic distance decreases in the gradual heating regime (from $T=0.2$ to 0.739). This means that atoms displace farther and farther away from their equilibrium sites and the vibrating atoms are getting closer momentarily, which was originally used by Lindemann in his melting criterion.[3] So the *shortest* interatomic distance among all atom pairs becomes smaller and smaller. In the isothermal heating regime before melting, the shortest distance is found to be about 0.89σ, which is still much larger than both $r_{oct\text{-}atom}=0.82\sigma$ and $r_{tet\text{-}atom}=0.71\sigma$. This result indicates that atoms have not occupied any interstitial sites before melting occurs. It is also worth mentioning that even after melting occurs, the shortest interatomic distance in liquid state is still about 0.89σ.

The next candidate is vacancy. Vacancy formation in crystals is closely related to the number of the first nearest neighbors. A missing neighbor of an atom would be a necessary sign for the formation of a nearby vacancy. Using the method outlined in Sec. II C, we have calculated the average number of the 1NNs as a function of time, as shown in Fig. 8. The heating process is the same as that shown in Fig. 2(b). At low temperatures, the 1NN number is exactly 12, indicating that the crystal has a perfect fcc structure. As the temperature increases, the thermal fluctuations displace atoms away from their equilibrium sites, so some atoms lose some of their 1NNs. After 0.25 ns (at $T=0.42$), the number starts to deviate from 12. After the temperature reaches the isothermal regime ($T=0.739$), the average number decreases to 11.7. In the quiescent period before melting, the average number remains at 11.7 with slight fluctuations. After melting occurs, the average number drops abruptly to 9.4.

Figure 9 shows five distributions of the number of the 1NNs at different times marked by A to E in Fig. 8. At time A ($T=0.2$), 100% of the atoms have 12 1NNs. At time B ($T=0.64$), about 75% of the atoms have 12 1NNs, about 16% of them have 11 1NNs, 8% of them have 13 1NNs, and 1% of them have 10 1NNs. This means that the crystal structure has some distortions at this temperature, but the fcc structure is still maintained. At time C ($T=0.739$, before melting occurs) and time D ($T=0.739$, when melting begins), the distributions are almost identical. About 52% of atoms have 12 1NNs. The percentages for the rest of the numbers are 1% for 9 1NNs, 9.5% for 10 1NNs, 28% for 11 1NNs, and 9.5% for 13 1NNs. At time E ($T=0.739$, after melting occurs), the distribution is very flat because the liquid is highly disordered. The number of the 1NNs ranges from 6 to 13 and the average number is about 9.4. From time D (crystal) to time E (liquid), the change in the distribution becomes very obvious during the melting transition. Thus, one can define, in a statistical sense, an atom with nine or less 1NNs (which is

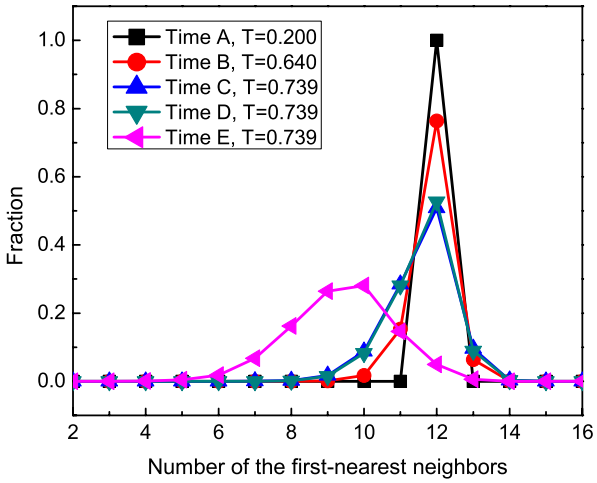

FIG. 9. (Color online) Distributions of the number of the first nearest neighbors at different times (marked by A–E in Fig. 8) during the isothermal melting process. time A: at $T=0.2$; time B: at $T=0.64$; time C: at $T=0.739$ and before melting occurs; time D: at $T=0.739$ and when melting occurs; time E: at $T=0.739$ and after melting occurs.

approximately the mean value for the liquid, see time E in Fig. 9) as a liquidlike atom.

A vacancy in the fcc structure corresponds to a missing atom from the lattice site, or a missing neighbor for the atoms surrounding the vacancy. If we follow this argument, the fraction of the vacancies is approximately 1/12 of the fraction of the atoms with a missing 1NN. At $T=0.739$ before melting, there are about 40% atoms that have less than 12 1NNs, which leads to the vacancy concentration of about 3%–4%. This concentration is at the same order of magnitude as those estimated for most metals at melting.[5] The experimental measurement of the vacancy concentration of copper[37] is only about 1.9×10^{-4}. However, the measurement was for heterogeneous melting and was performed at temperatures below the equilibrium melting point. In the heterogeneous melting, the presence of surface suppresses the formation of vacancies inside the crystal. Thus, this measurement cannot be used as the reference for homogeneous melting. To the best of our knowledge, no experimental measurement is available yet for homogeneous melting.

On the other hand, to form a vacancy in a perfect crystal without surface (if the crystal has surface or interface, the atoms can escape to these places), an interstitial should also be present. The lack of interstitials as seen in this work suggests that the so-called vacancies as we mentioned in last paragraph may consist mainly of the open spaces in the superheated crystal in the form of some transient disorder. These open spaces cannot be classified as the vacancies defined conventionally that have long lifetimes. As mentioned in Sec. II C, we define this kind of transient open space as the dynamic 1NN disorder. The dynamic 1NN disorder gives rise to the missing neighbor on a statistical sense as measured from the distributions over a short period of time (Fig. 9) and plays an important role in homogeneous melting.

D. Self-diffusion rings or loops

By far, we have established the following important results from a superheated crystal before melting: (1) the presence of open spaces, including the dynamic 1NNs and vacancies; (2) the diffusive motions involving atom hopping to neighboring lattice sites while the crystal lattice remains largely intact; and (3) the subsequent evolution of the atoms in this environment leads to homogeneous melting. Since the atom hopping is closely related to destroying the stability of the crystal, it is reasonable to expect that it is the diffusive motion that eventually leads to liquid phase nucleation and melting. In the following, we will further illuminate this process with a particular emphasis on establishing its relation with homogeneous melting. For clear visualization, in this section, we use a smaller system of 500 atoms at the isothermal temperature of 0.725. Note that in the gradual heating, the upper superheating limit T_m^s is at about 0.76 for different size systems. In the isothermal heating, however, the smaller system can melt at a lower temperature in the isothermal regime. The system of 500 atoms melts at 0.725, while a system of 4000 atoms melts at 0.739. This is because the smaller system has larger thermal fluctuations and is more vulnerable to distortions during the isothermal heating. When the number of atoms is greater than 4000, the finite-size effects become insignificant and the isothermal melting temperature approaches 0.740.

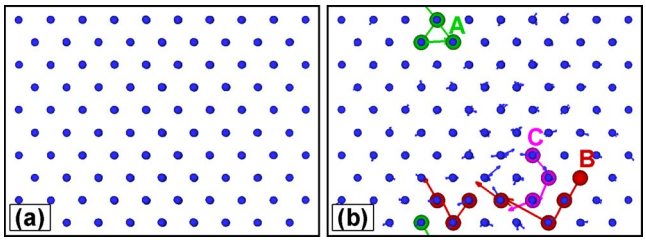

FIG. 10. (Color online) Atom hopping in a crystal consisting of 500 atoms during the isothermal heating. The snapshots are 2D projections along the [110] direction. The smaller spheres in blue (black) represent the equilibrium atom positions. The bigger spheres in other colors represent hopping atoms. (a) Equilibrium atom positions and (b) clusters (indicated by bigger atoms) formed by the atom hopping. The vectors connect the equilibrium and new positions. The arrowheads of the vectors mark the new atom positions.

When the temperature reaches the isothermal heating regime at 0.725, the position of each atom is averaged over the first 0.025 ns (5000 MD steps) period to get the equilibrium positions, which are used as the reference positions throughout the isothermal heating simulation. In Fig. 10(a), we show the 2D projection of the equilibrium or reference atomic positions projected along [110] direction. The atoms are represented by small blue (black) spheres. Apparently, the atomic positions at the beginning of the isothermal heating are well ordered and form a nearly perfect fcc lattice. Next, we mapped out the atomic trajectories, which are done by averaging the position of each atom over every 100 MD steps (0.5 ps). Here, we use the "averaged" positions instead of "instantaneous" ones because the former are relatively free of the "noises" from thermal fluctuations. As time elapses in the isothermal regime, the thermal fluctuations cause atoms to wander away. Figure 10(b) shows the atomic displacements after 2.65 ns from the beginning of the isothermal heating. For visualization purpose, we still use small blue

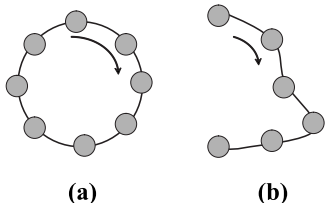

FIG. 11. Schematic illustrations of two types of diffusion loops. (a) A closed diffusion loop and (b) an open diffusion loop.

spheres to show the equilibrium positions as we did in Fig. 10(a). However, the new atom positions are not shown with spheres. Instead, we use vectors to connect the new atom positions and the equilibrium positions. Therefore, in Fig. 10(b), the actual new atom positions are at the arrowheads of the vectors. Using this way, we can clearly see how far the atoms displace from their equilibrium positions and which atoms become disordered. One can see that most atoms only displace slightly around their equilibrium positions. However, a few atoms clearly become diffusive and their displacements are about one nearest-neighbor distance, which is in good agreement with the prediction drawn from Fig. 6. In other words, these atoms have hopped to their neighboring lattice sites. To make these atoms more visible, we use bigger spheres to represent them. The extraordinary large magnitude of the MSD seen in Fig. 5(b) is mainly caused by this kind of atom hopping in the isothermal regime.

Figure 10(b) also shows that the atom hopping occurs in a *collective* way. Since there are no preformed vacancies in the superheated crystal, a hopping atom needs to "kick" a neighboring atom away in order to occupy its lattice site, or to put it differently, to take advantage of the open space formed at the neighboring atom. The neighboring atom also needs to kick the third atom away, and so forth. As a result, these atoms form a diffusion ring or diffusion loop. This formation of the diffusion loops only requires some short-lived open spaces, or dynamic 1NN disorder. In Fig. 10(b), the atoms belonging to the same loop are shown with the same color.

There are two types of the diffusion loops, closed loop and open loop, as illustrated in Fig. 11. In the closed loop, each atom displaces one first-nearest-neighbor distance. After the hopping completes, the original lattice site of the first hopping atom is occupied by the last hopping atom. Thus, there is no vacancy, or other permanent disorder, left in the crystal after the loop forms completely. Clearly, the closed loops do not cause topological disorder to the lattice (or melting), because atoms in the closed loops have already finished hopping from lattice to lattice sites. However, they contribute a large fraction to the MSD as shown in Fig. 5(b). In the open loop, the first hopping atom leaves an open space, or a dynamic 1NN disorder, and the last atom moves less than one nearest-neighbor distance from its initial lattice site. For example, loop A in Fig. 10(b) is a closed loop (note that the bottom atom in green color is part of this loop due to the periodic boundary conditions), while loops B and C are open loops. An open loop can also be considered as being in a transient state of forming a closed loop.

The detailed process of the loop formation can be seen from four snapshots in Fig. 12. The pictures are tilted slightly

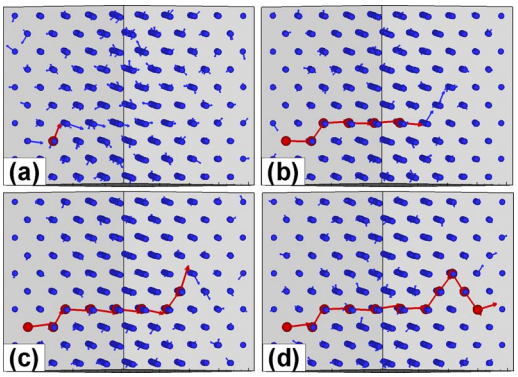

FIG. 12. (Color online) Four snapshots of forming a diffusion loop. The viewing angle is tilted slightly from the [110] direction. The blue (black) spheres represent original equilibrium sites. The red (dark gray) spheres represent the hopping atoms. The vectors represent the atom displacements and the arrowheads indicate the new atom positions. (a) At the beginning of forming a loop, (b) after 1.6 ps, (c) after 4.4 ps, and (d) after 6.1 ps.

for better visualization. In all snapshots, the spheres (both red and blue) represent the original equilibrium atom positions at the beginning of the isothermal regime. The blue spheres represent nonhopping atoms, and the red spheres represent hopping atoms. The new atom positions are at the arrowheads of the vectors. As shown in Fig. 12(a), initially an atom (indicated by red color) moves to one of its nearest neighboring sites. We define the first hopping atom as the head atom of the loop. The atom at that neighbor site is "pushed" away, or "moved" away, as indicated by the long blue vectors. In addition, another atom tends to fill the open space created by the first hopping atom. After 1.6 ps, six atoms have hopped from their initial positions, as shown in Fig. 12(b). The six atoms form a transient or open loop while the crystal lattice remains intact. The two atoms in blue color near the end (the sixth hopping atom) of the loop have already moved away from their original positions but have not arrived at the new lattice sites yet. After 4.4 ps, eight atoms have hopped from their initial positions, as shown in Fig. 12(c). After 6.1 ps, 11 atoms have hopped away from their initial positions, as shown in Fig. 12(d). Due to the periodic boundary conditions, the 11 atoms form a closed loop. From this process, we can estimate the average time of one atom hopping, which is about $6.1\ \text{ps}/11 \approx 0.55$ ps. Using systems of different sizes, we found that the number of atoms in a diffusion loop depends on the sample size. It could be as small as a few atoms in small systems and as big as a few hundred atoms in large systems. This is because the diffusion loops can percolate across the entire system. Therefore, it is not surprising to find bigger diffusion loops in a larger system.

E. Homogeneous melting caused by ring diffusion

Without preexisting defects or surfaces in a perfect crystal, melting must nucleate from internal defects caused by thermal agitation. In Sec. III C, we have ruled out the possibility of forming interstitials in perfect fcc crystals. Instead,

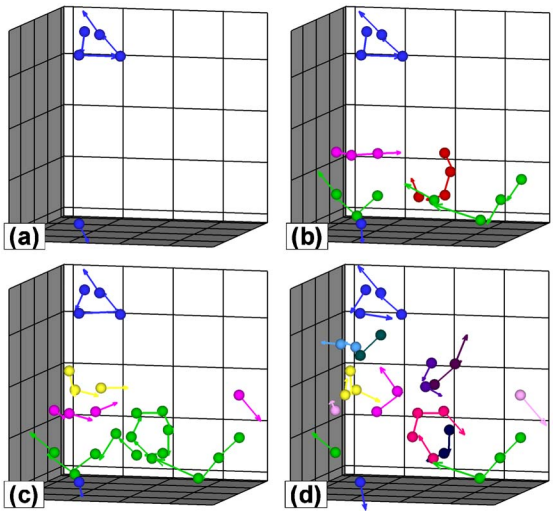

FIG. 13. (Color online) Three-dimensional snapshots of the diffusion loops during the isothermal melting process. In order to illustrate the diffusion loops more clearly, only the atoms in the diffusion loops are shown. Different loops are distinguished by different colors. (a) At $t=0$ (the beginning of isothermal regime), (b) after 7.0 ps, (c) after 9.0 ps, and (d) after 9.2 ps.

we observed enhanced self-diffusion at elevated temperatures. The atomic motions take place predominantly in the form of self-diffusion ring or loop in which the atoms hop to its nearby lattices with the help of the thermally agitated open spaces, or dynamic 1NN disorder. In the following, we show that it is the hopping atoms that cause nucleation of the liquid phase and thus the homogeneous melting when they reach a critical number density.

The evolution of the diffusion loops at $T=0.725$ in a system of 500 atoms is shown with four three-dimensional snapshots in Fig. 13. For clear visualization, only the hopping atoms are shown. As same as in Fig. 10, the spheres represent the initial equilibrium atom positions, and the vector pointing from each atom indicates the displacement direction of that atom. The new atom positions are at the arrowheads of vectors. Figure 13(a) shows a closed diffusion loop in which each atom moves one nearest-neighbor distance. After the closed loop forms, the hopping stops and all the atoms in the loop vibrate around their new positions. Thus, the closed loop does not affect the stability of the crystal *after* the loop completes. After 7 ps, three new diffusion loops appear, as shown in different colors in Fig. 13(b). The three new loops are all open loops. In addition, the loop in green color and the loop in red color are very close to each other. The closed loop shown in Fig. 13(a) is still there, indicating that the atoms in this loop did not make further hopping within this time period. Note that it is possible for the atoms in closed loops to hop again later, and there is no history effect on the future hopping: A previously hopping atom does not have the advantage or disadvantage for a new jump. After additional 2 ps, the green and red loops shown in Fig. 13(b) joined to form a single loop, which is shown in green color in Fig. 13(c). However, just 0.2 ps after the two open loops merge to one loop, it collapses and some new small open loops appear, as shown in Fig. 13(d). At this moment, the system starts to melt. Thus, it seems that the interaction of open loops can cause instability to the system. On the other hand, one can also find that the closed loop in Fig. 13(a) is stable throughout the nucleation process. Thus, the closed loop does not destabilize the system.

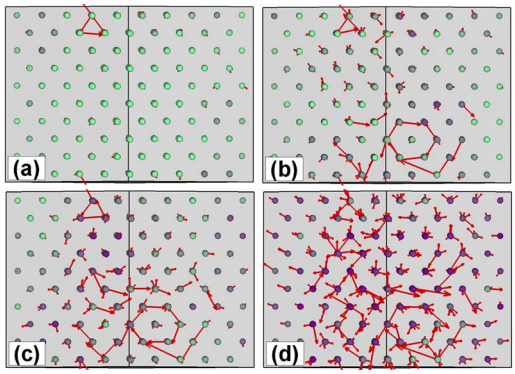

FIG. 14. (Color online) Enthalpy change of each atom during the formation of the diffusion loops. Each sphere is colored according to its enthalpy. The bright green (light gray) is for low enthalpy (solidlike) atoms and the dark purple (dark gray) is for high enthalpy (liquidlike) atoms. The vectors represent the atom displacements and the arrowheads represent the actual atom positions. (a) At $t=0$, (b) after 7.0 ps, (c) after 9.0 ps, and (d) after 9.2 ps.

The connection between the open loops and liquid nucleus formation can be further illuminated through the enthalpy change of atoms. When atoms become disordered or lose some neighbors, their enthalpies increase. If the enthalpy of an atom is high, it is more liquidlike, and vice versa.[25] At each stage shown in Fig. 13, we calculated the enthalpy of each atom averaged over every 0.5 ps (100 MD steps). Then, each atom is colored according to its individual enthalpy in the snapshots. The color continuously changes from bright green (for solidlike atoms) to dark purple (for liquidlike atoms). The details of the coloring scheme can be found in our previous work.[25,38] In Fig. 14, we show the corresponding snapshots projected along the [110] direction. In Fig. 14(a), most spheres are in light green color, which means that these atoms are more solidlike. One also can find that the atom displacements are very small, and the atoms in the closed loop are also solidlike ones. In Fig. 14(b), some atoms displace away from their equilibrium sites. It can be clearly seen that most displaced atoms (especially the atoms in the open loops) are in dark green colors, indicating that these atoms are in the intermediate state between the solid and liquid. In Fig. 14(c), more displaced atoms appear and some of them are in dark purple color, indicating that they become liquidlike atoms. In Fig. 14(d), almost all atoms displace largely away from their equilibrium sites. At the mean time, the colors of these atoms are close to dark purple, indicating that they become liquidlike atoms. Therefore, the displaced atoms coincide with the atoms of high enthalpies. In other words, the liquidlike atoms prefer to appear and grow at or in the vicinity of the open diffusion loops.

In open loops, atoms move in an asynchronized fashion. The head, or the first hopping atom in an open loop, leaves an open space behind it. The tail, or the last moving atom in the loop, displaces away from its original position but has

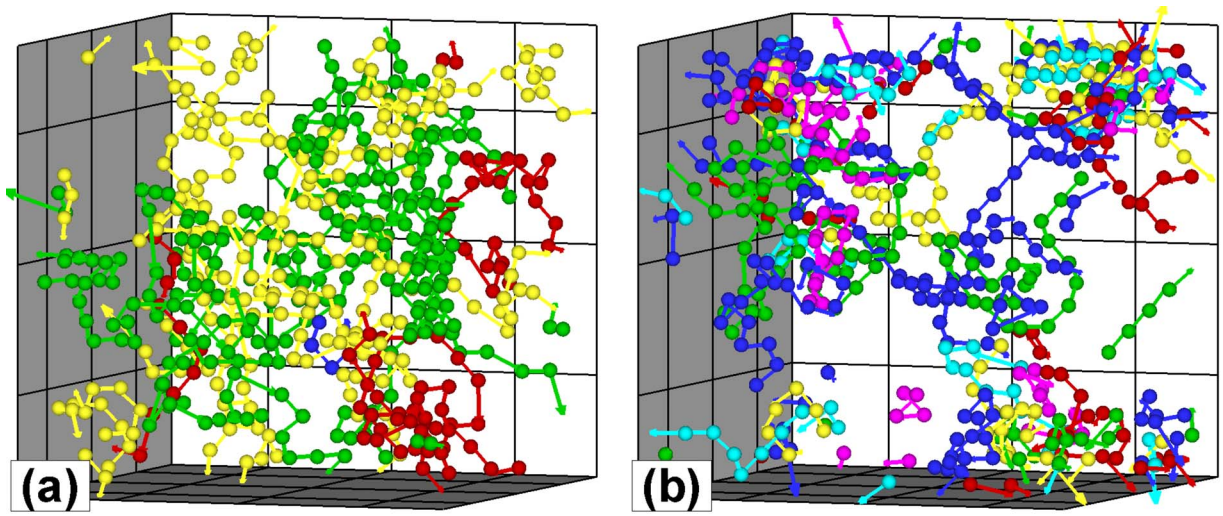

FIG. 15. (Color online) Open diffusion loops in a system of 4000 atoms at two isothermal temperatures: (a) $T=0.738$ and (b) $T=0.739\varepsilon/k_B$. Atoms in the same color belong to the same loop.

not arrived at the new position yet. The other atoms in the open loop have hopped to their neighboring sites. Thus, the head and tail positions in an open loop are most potent to cause the instability to the crystal. In order to cause sufficient disorder to nucleate a liquid phase, certain density of the head and tail atoms (or open loops) is needed. The number density is defined as the fraction of the number of these atoms, which is twice of the number of open loops, to the number of atoms in the system.

As an example, we have investigated the density of these atoms in a system consisting of 4000 atoms at both $T=0.738$ and $T=0.739$. The crystal does not melt at $T=0.738$ but does at $T=0.739$ within the time period of 4.5 ns. At both temperatures, extensive self-diffusion takes place and the corresponding snapshots of the open diffusion loops are shown in Fig. 15. Although many atoms have made hopping at $T=0.738$ [Fig. 15(a)], there are only three open loops and each loop is very long (consisting of a few hundred atoms). At $T=0.739$ [Fig. 15(b)], there are more open loops, which means that there are more head and tail atoms. So the system is less stable at this temperature. We have calculated the time evolution of the number of open loops at both temperatures, as shown in Fig. 16(a). Note in this graph the time is scaled to zero when the temperature is in the isothermal regime. At $T=0.738$, the number of the open loops is usually less than 10. At $T=0.739$, the number of the open loops is around 5 before melting occurs but increases rapidly when melting occurs. Figure 16(b) shows the zoom-in view during the short transition period at $T=0.739$. Before melting occurs, the number of the open loops is 21. One can also find that if the number is greater than 43, the system melts very quickly. So the number of 43 can be viewed as the upper bound of the critical number of the open loops, and the number of 21 can be viewed as the lower bound. Since each open loop has two defective atoms (head and tail), the upper bound of the critical density of unstable atoms is 0.022 and the lower bound is 0.011. Using this method, we have estimated the critical densities of the defective atoms in the systems of different sizes, $N=500$, 864, 1372, 2048, 2916, and 4000, and the result is shown in Fig. 17. One can find that the average upper bound of the critical density of defective atoms is around 1.8%, and the lower bound of the critical density is around 1.1%. So, in general, we estimate that the critical fraction of the defective atoms to cause homogeneous melting is about 1%–2%.

IV. DISCUSSION AND CONCLUSIONS

As mentioned in the Introduction, the main obstacle in our understanding of homogeneous melting in the superheating regime comes from the omnipresence of the surfaces, other crystal defects, and the fast transition dynamics in the superheating regime. The fast heating rate employed in computer simulations, and in experiments as well, imposes a strict kinetic constraint on phase space sampling, which causes strong hysteresis in homogeneous melting and suppression of

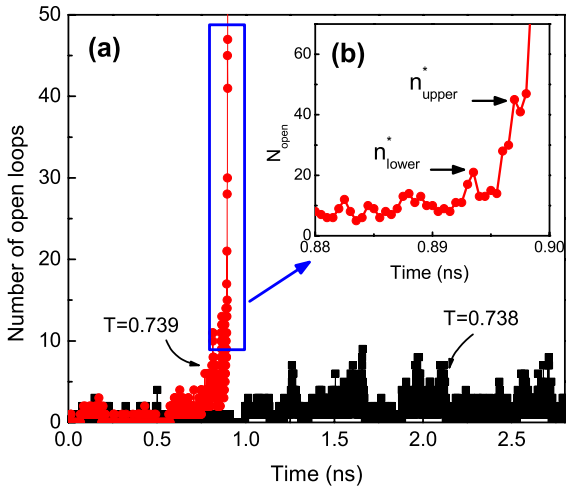

FIG. 16. (Color online) Evolution of the number of open loops at two isothermal temperatures. (a) Overall evolutions at $T=0.738$ and $T=0.739$ and (b) zoom-in view of the transition period enclosed by the blue rectangle.

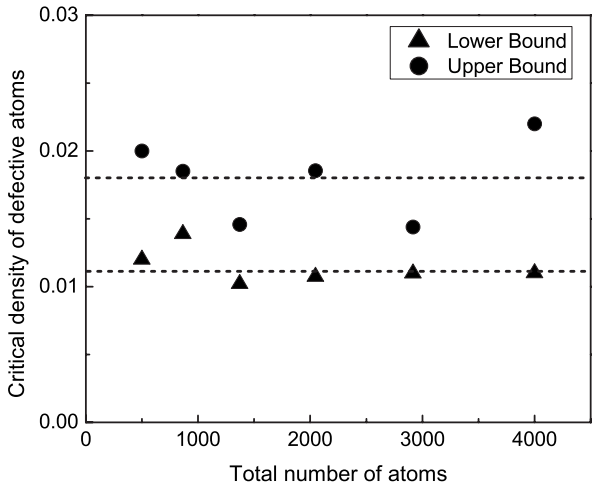

FIG. 17. Upper and lower bounds of the critical densities of defective atoms in various size systems.

kinetic process. As a result, the system is ushered to the superheating limit T_m^S and homogeneous melting becomes a catastrophic transition. Using the isothermal heating method, in conjunction with various characterization techniques, we are able to study homogeneous melting with a particular focus on atomic mechanisms in the superheating regime. The results suggest that it is a thermodynamic transition triggered by self-diffusion loops. The nucleation of liquid nuclei is directly related to the critical number density of the dynamic 1NN disorders which appear at and around the ends of the open loops. The kinetic behavior involving self-diffusion loops is not entirely a surprise as it may be the most efficient way to move atoms in a perfect crystal.

In light of these findings, we revisit some theoretical models proposed earlier and are able to make some remarks: (1) As we showed, homogeneous melting involves considerable diffusive atomic motions to nucleate the liquid phase. The Lindemann criterion,[3,16] which is based on the mean-square-displacement from the lattice vibration, is inadequate in explaining homogeneous melting in the superheating regime when the heating rate is slow, or for a thermodynamic transition. (2) Interstitial mediated melting[20,30–34] is unlikely due to the high formation energy in one-component fcc crystals. Similarly, the thought of vacancy mediated homogeneous melting may be shadowed by the overwhelming 1NN dynamic disorder, which may appear like vacancies but with very short lifetime. (3) Despite certain geometric similarities, the self-diffusion loops are not dislocation loops or dislocation lines[17,27–29] that have been hypothesized as the major defects to cause melting. The self-diffusion loops do not possess the characteristic atomic structures and strain fields of dislocations. In addition, the collective motion in dislocations involves other atoms on the atomic planes either perpendicular or parallel to the defect lines. However, in diffusion loops, such a feature does not exist. (4) The nature of being a first-order transition allows us to revise some previous predictions. For example, Born perceived that melting is caused by the elastic instability with the gradual vanishing of a shear modulus at the transition.[2] However, the nucleation-and-growth model[36] of the first-order melting confirmed in this work predicts that the elastic modulus should be finite at melting, even at the superheating limit.[16,20,21,39]

The atomistic simulation results also provide a basis for the formulation of a thermodynamic understanding of homogeneous melting. As a result, we can cast the transition in a classical nucleation theory.[40] Conversely, the thermodynamic formulation allows us to consider variables and factors that are difficult to obtain directly from atomistic simulations, such as the interface energy,[25] internal elastic energy caused by the volume change at melting,[36] and curvature effect at the liquid-solid interface.[38] The complement of these works at different length scales has led to a deeper understanding of melting at superheating regime.

ACKNOWLEDGMENTS

The financial support of this work was provided by the Structural Amorphous Metals Program of DARPA under ARO Contract No. DAAD19-01-1-0525. X.-M.B. is grateful for a support provided by Georgia Tech where the current work was performed during his Ph.D. study.[39]

*Present address: Department of Chemical and Biological Engineering, Northwestern University, Evanston, Illinois 60208-3120; xmbai@northwestern.edu
†Corresponding author; ml190@mail.gatech.edu

[1] D. A. Porter and K. E. Easterling, *Phase Transformations in Metals and Alloys* (Chapman & Hall, London, 1992).
[2] M. Born, J. Chem. Phys. **7**, 591 (1939).
[3] F. A. Lindemann, Phys. Z. **11**, 609 (1910).
[4] R. W. Cahn, Nature (London) **273**, 491 (1978).
[5] H. J. Fecht and W. L. Johnson, Nature (London) **334**, 50 (1988).
[6] J. L. Tallon, Nature (London) **342**, 658 (1989).
[7] J. W. M. Frenken and J. F. van der Veen, Phys. Rev. Lett. **54**, 134 (1985).
[8] P. Stoltze, J. K. Norskov, and U. Landman, Phys. Rev. Lett. **61**, 440 (1988).
[9] J. Daeges, H. Gleiter, and J. H. Perepezko, Phys. Lett. A **119**, 79 (1986).
[10] S. Williamson, G. Mourou, and J. C. M. Li, Phys. Rev. Lett. **52**, 2364 (1984).
[11] V. I. Motorin and S. L. Musher, J. Chem. Phys. **81**, 465 (1984).
[12] K. Sokolowski-Tinten, C. Blome, C. Dietrich, A. Tarasevitch, M. Horn von Hoegen, D. von der Linde, A. Cavalleri, J. Squier, and M. Kammler, Phys. Rev. Lett. **87**, 225701 (2001).
[13] B. Rethfeld, K. Sokolowski-Tinten, D. von der Linde, and S. I. Anisimov, Phys. Rev. B **65**, 092103 (2002).
[14] B. J. Siwick, J. R. Dwyer, R. E. Jordan, and R. J. D. Miller, Science **302**, 1382 (2003).
[15] K. Lu and Y. Li, Phys. Rev. Lett. **80**, 4474 (1998).
[16] Z. H. Jin, P. Gumbsch, K. Lu, and E. Ma, Phys. Rev. Lett. **87**, 055703 (2001).

[17] L. Gomez, A. Dobry, C. Geuting, H. T. Diep, and L. Burakovsky, Phys. Rev. Lett. **90**, 095701 (2003).
[18] S. N. Luo, T. J. Ahrens, T. Cagin, A. Strachan, W. A. Goddard, and D. C. Swift, Phys. Rev. B **68**, 134206 (2003).
[19] S. N. Luo, A. Strachan, and D. C. Swift, J. Chem. Phys. **120**, 11640 (2004).
[20] M. Forsblom and G. Grimvall, Nat. Mater. **4**, 388 (2005).
[21] Q. S. Mei and K. Lu, Prog. Mater. Sci. **52**, 1175 (2007).
[22] M. Parrinello and A. Rahman, J. Appl. Phys. **52**, 7182 (1981).
[23] S. Nose, Mol. Phys. **52**, 255 (1984).
[24] M. P. Allen and D. J. Tildesley, *Computer Simulation of Liquids* (Clarendon, New York, 1987).
[25] X. M. Bai and M. Li, J. Chem. Phys. **124**, 124707 (2006).
[26] A. B. Belonoshko, R. Ahuja, O. Eriksson, and B. Johansson, Phys. Rev. B **61**, 3838 (2000).
[27] L. Burakovsky, D. L. Preston, and R. R. Silbar, Phys. Rev. B **61**, 15011 (2000).
[28] F. Delogu, J. Phys. Chem. B **109**, 15291 (2005).
[29] F. Lund, Phys. Rev. Lett. **69**, 3084 (1992).
[30] M. Forsblom and G. Grimvall, Phys. Rev. B **72**, 054107 (2005).
[31] A. V. Granato, Phys. Rev. Lett. **68**, 974 (1992).
[32] Y. J. Zhou and X. F. Jin, Phys. Rev. B **71**, 224113 (2005).
[33] K. Nordlund and R. S. Averback, Phys. Rev. Lett. **80**, 4201 (1998).
[34] K. Nordlund, Y. Ashkenazy, R. S. Averback, and A. V. Granato, Europhys. Lett. **71**, 625 (2005).
[35] C. Kittel, *Introduction to Solid State Physics* (Wiley, New York, 1996).
[36] X. M. Bai and M. Li, Phys. Rev. B **72**, 052108 (2005).
[37] R. O. Simmons and R. W. Balluffi, Phys. Rev. **129**, 1533 (1963).
[38] X. M. Bai and M. Li, Nano Lett. **6**, 2284 (2006).
[39] X. M. Bai, Ph.D. thesis, Georgia Institute of Technology, 2006.
[40] X. M. Bai and M. Li, J. Chem. Phys. **123**, 151102 (2005).